

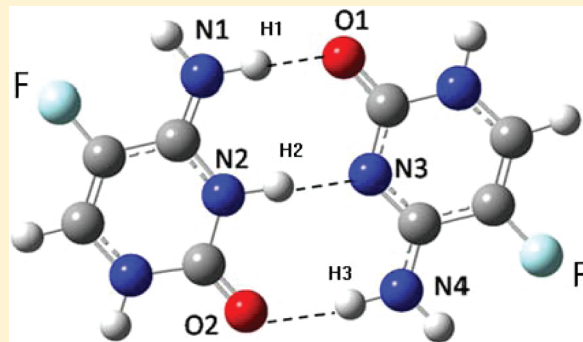
# Tridentate Ionic Hydrogen-Bonding Interactions of the 5-Fluorocytosine Cationic Dimer and Other 5-Fluorocytosine Analogues Characterized by IRMPD Spectroscopy and Electronic Structure Calculations

Sabrina M. Martens,\* Rick A. Marta, Jonathan K. Martens, and Terry B. McMahon\*

Department of Chemistry, University of Waterloo, 200 University Avenue, Waterloo, Ontario N2L 3G1, Canada

 Supporting Information

**ABSTRACT:** Ionic hydrogen-bonding interactions have been found in several clusters formed by 5-fluorocytosine (5-FC). The chloride and trimethylammonium cluster ions, along with the cationic (proton-bound) dimer have been characterized by infrared multiple-photon dissociation (IRMPD) spectroscopy and electronic structure calculations performed at the B2PLYP/aug-cc-pVTZ//B3LYP/6-311+G(d,p) level of theory. IRMPD action spectra, in combination with calculated spectra and relative energetics, indicate that it is most probable that predominantly a single isomer exists in each experiment. For the 5-FC-trimethylammonium cluster specifically, the calculated spectrum of the lowest-energy isomer convincingly matches the experimental spectrum. Interestingly, the cationic dimer of 5-FC was found to have a single energetically relevant isomer (Cationic-IV) involving a tridentate ionic hydrogen-bonding interaction. The three sites of intermolecular ionic hydrogen bonds in this isomer interact very efficiently, leading to a significant calculated binding energy of 180 kJ/mol. The magnitude of the calculated binding energy for this species, in combination with the strong correlation between the simulated and IRMPD spectra, suggests that a tridentate-proton-bound dimer was observed predominantly in the experiments. Comparison of the calculated relative Gibbs free energies (298 K) for this species and several of the other isomers considered also supports the likelihood of the dominant protonated dimer existing as Cationic-IV.



## INTRODUCTION

The pyrimidine 5-fluorocytosine (5-FC) is a fluorinated analogue of the DNA nucleobase cytosine. 5-FC (also known as flucytosine or the drug Ancobon) is the single antifungal agent available that can act as an antimetabolite drug.<sup>1</sup> Its mechanism of action has been debated over the years and has been considered to be a combination of two or more processes that interfere with pyrimidine metabolism.<sup>2–4</sup> Conversion of 5-fluorocytosine to 5-fluorouracil can occur by means of deamination within the fungal cells.<sup>5</sup> Two main mechanisms have been proposed, one in which an analogue of 5-fluorouracil, fluorodeoxyuridine monophosphate (FdUMP), functionally inhibits the enzyme thymidylate synthase, the sole source of de novo synthesis of thymine in the body,<sup>6</sup> and another in which 5-fluorouridine triphosphate (FURTP) is incorporated in place of uridylic acid in the fungal RNA, disrupting subsequent protein and carbohydrate synthesis.<sup>4</sup>

5-Fluorocytosine has also been used in recent cancer research involving suicide gene therapy, in what is considered to be an experimental approach to tumor cell death. This method has been shown to activate 5-fluorocytosine to the anticancer agent 5-fluorouracil inside the tumor, where 5-fluorouracil can carry out its mechanism of thymidylate synthase inhibition and lead to

the inhibition of DNA synthesis and tumor growth.<sup>7</sup> In other similar studies, replicating retrovirus vectors have been used and enhanced by the addition of prodrugs such as 5-fluorocytosine, which have led to more effective tumor-selective cell death.<sup>8</sup>

In this study, 5-fluorocytosine has been investigated by infrared multiple-photon dissociation (IRMPD) spectroscopy and modern electronic structure calculations. Understanding the nature of structures and interactions of gaseous ionic species formed by 5-FC can permit predictions to be made about the intrinsic reactivity of the molecule. Modeling biologically relevant molecules in the gas phase allows for highly relevant information to be determined because of the many hydrophobic environments found in the body. IRMPD is a powerful and sensitive technique that has proved to be highly valuable in structural elucidation studies of gaseous ions.<sup>9–14</sup> IR spectral signatures suggest the presence of ionic hydrogen-bond interactions in cluster ions of 5-fluorocytosine with trimethylammonium (TMA) and chloride, in addition to the cationic homodimers formed by this species.

**Received:** February 15, 2011

**Revised:** July 10, 2011

**Published:** July 14, 2011

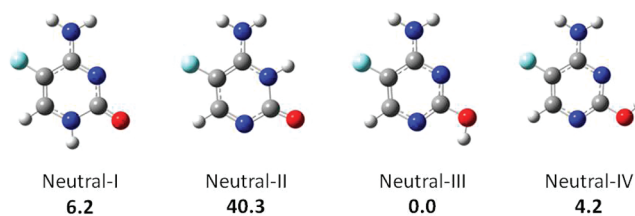


**Figure 1.** Structures and relative Gibbs free energies (298 K) of several isomers of 5-fluorocytosine. Structures were optimized at the B3LYP/6-311+G(d,p) level of theory, and relative Gibbs free energies (kJ/mol) were calculated at the B2PLYP/aug-cc-pVTZ//B3LYP/6-311+G(d,p) level of theory.

## ■ EXPERIMENTAL SECTION

IRMPD experiments were performed using the infrared free electron laser (IR-FEL) at the Centre de Laser Infrarouge d'Orsay (CLIO) facility in Orsay, France. The IR-FEL beam was directed into a Bruker Esquire 3000+ ion-trap mass spectrometer, equipped with an electrospray ionization interface. Similar experimental setups have been described in detail elsewhere.<sup>11,15–18</sup> The IR-FEL beam is created by emission from a 10–50 MeV electron beam that passes through the gap between a set of periodic undulator magnets. By adjusting the undulator gap, the emission photon wavelength is able to be tuned through the mid-infrared range. The undulator is held within a 4.8-m-long optical cavity. The laser beam is accumulated in an optical cavity, and out-coupling is permitted through a 1–3-mm hole in one of two silver mirrors, each with a diameter of 38 mm.

The work described here involved the use of electron energies of 46 MeV, which permitted continuous scans over a frequency range of 1000–1900 cm<sup>-1</sup>. The IR-FEL output consists of a train of 8-μs macropulses, with a repetition rate of 25 Hz. Each macropulse consists of approximately 500 micropulses, with a width of a few picoseconds per pulse. For an average IR power of 500 mW, the corresponding micropulse and macropulse energies are about 40 μJ and 20 mJ, respectively.

Stock solutions of 5-fluorocytosine were prepared by combining a 20:80 mixture of water and acetonitrile with 5 mg of 5-fluorocytosine to a total volume of 8 mL. Subsequently, potassium chloride or trimethylammonium chloride was added for the experiments involving 5-fluorocytosine–chloride (5-FC–Cl) and –trimethylammonium (5-FC–TMA) clusters, respectively. Ions were supplied from these solutions ( $10^{-6}$ – $10^{-4}$  M) using an electrospray ionization interface. The ionic species of interest were then isolated and restricted within the quadrupole ion-trap mass spectrometer, and the IR-FEL beam was focused and introduced into the center of the ion trap. Following the laser irradiation, consequence mass spectra were recorded, and an accumulation of 10 spectra was obtained for each wavelength. IRMPD spectra were acquired by scanning the wavelength in steps of approximately 4 cm<sup>-1</sup>. The spectra reported here are expressed in terms of the fragmentation efficiency,  $P_{\text{frag}}$ , as a function of the photon energy (in cm<sup>-1</sup>)

$$P_{\text{frag}} = -\log \left( \frac{I_{\text{parent}}}{\sum I_{\text{fragment}} + I_{\text{parent}}} \right) \quad (1)$$

where  $I_{\text{parent}}$  and  $\sum I_{\text{fragment}}$  are the intensity of the parent ion and the sum of the intensities of the fragment ions, respectively.

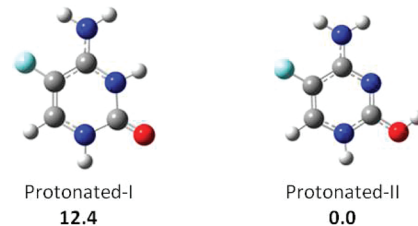


**Figure 2.** Structures and relative Gibbs free energies (298 K) of isomers of protonated 5-fluorocytosine. Structures were optimized at the B3LYP/6-311+G(d,p) level of theory, and relative Gibbs free energies (kJ/mol) were calculated at the B2PLYP/aug-cc-pVTZ//B3LYP/6-311+G(d,p) level of theory.

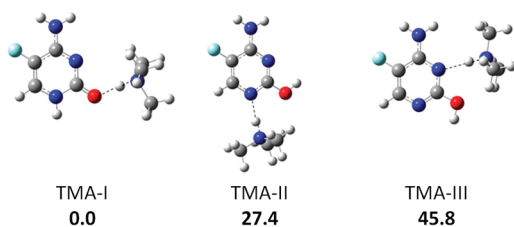


**Figure 3.** Structures and relative Gibbs free energies (298 K) of several isomers of the 5-fluorocytosine–trimethylammonium cluster. Structures were optimized at the B3LYP/6-311+G(d,p) level of theory, and relative Gibbs free energies (kJ/mol) were calculated at the B2PLYP/aug-cc-pVTZ//B3LYP/6-311+G(d,p) level of theory.

Comparison of vibrational signatures found in the IRMPD spectrum with the calculated spectra allowed several structural determinations to be made. It is important to note that, according to this approach, the relative intensities between the calculated and experimental spectra will vary. Because unimolecular dissociation of the parent ion relies on having sufficient energy in the mode corresponding to the reaction coordinate, the intensity of the experimental spectrum is dependent on the intramolecular vibrational energy redistribution (IVR) efficiency of the species, in addition to the laser power, which can be subject to some fluctuations. The calculated vibrational spectrum is based on the absorption intensities of vibrational modes for the species and does not account for the IVR process or for fluctuations in laser power.

## ■ ELECTRONIC STRUCTURE CALCULATIONS

Electronic structure calculations were performed using the Gaussian 03 and 09 software packages.<sup>19,20</sup> Structures of the 5-fluorocytosine analogues were optimized using the density functional theory (DFT) method B3LYP, along with the 6-311+G(d,p) basis set. A frequency scaling factor of 0.9679 was used to account for systematic errors arising from the use of calculated harmonic frequencies and also any long-range electron correlation effects.<sup>21–27</sup> The B3LYP method in combination with the 6-311+G(d,p) basis set has been shown to be a reliable level of theory with a good compromise between accuracy and cost for smaller systems such as those described here.<sup>12,17,28</sup> In addition, this level of theory has previously been shown to produce theoretically generated infrared spectra that approximate IRMPD spectra adequately and has also been shown to outperform other DFT methods, as well as some MP2 calculations.<sup>18,29</sup> All geometry optimizations were performed using “tight” force displacement (opt=tight) and energy convergence (scf=tight) specifications. To better approximate electronic energies, single-point

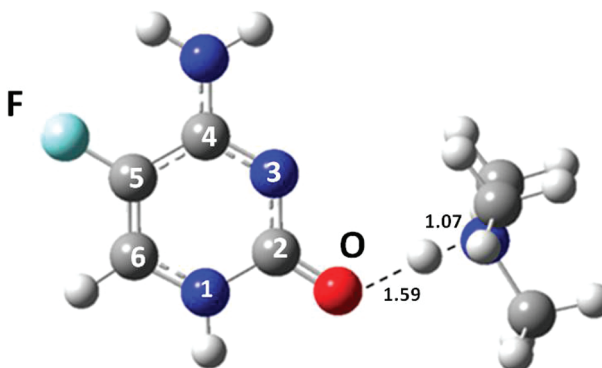
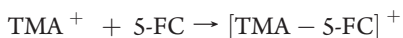


**Figure 4.** Structure of the lowest-energy trimethylammonium–5-FC isomer, TMA-I, calculated at the B3LYP/6 + 311+G(d,p) level of theory. The ionic hydrogen bond is represented as a black dotted line. Bond lengths are in units of angstroms (Å).

**Table 1.** Thermochemical Values (298 K) for the Formation of Several Isomers of the Trimethylammonium–5-FC Complex Calculated at the B2PLYP/aug-cc-pVTZ//B3LYP/6-311+G(d,p) Level



reaction scheme	$\Delta H^\circ$ (kJ/mol)	$\Delta S^\circ$ [J/(mol K)]	$\Delta G^\circ$ (kJ/mol)
$\text{TMA}^+ + \text{Neutral-I} \rightarrow \text{TMA-I}$	-140	-139	-98.7
$\text{TMA}^+ + \text{Neutral-IV} \rightarrow \text{TMA-II}$	-113	-146	-69.3
$\text{TMA}^+ + \text{Neutral-III} \rightarrow \text{TMA-III}$	-86.5	-133	-46.8

calculations were performed at the B2PLYP/aug-cc-pVTZ level of theory on all B3LYP-optimized geometries.

Harmonic fundamental frequencies determined by ab initio and DFT self-consistent field (SCF) methods are known to overestimate experimental fundamental frequencies for covalently bound molecules by 8–12%. The reasons for such overestimations are basis set incompleteness, electron correlation effects, and anharmonicity.<sup>30</sup> Anharmonic frequencies can be obtained by treating cubic and quartic potentials as perturbations to a harmonic oscillator potential. The anharmonic potential requires numerical evaluation of higher-order partial derivatives to obtain anharmonic force constants. Evaluation of such higher-order partial derivatives by Gaussian<sup>19,20</sup> results in anharmonic frequencies being significantly more costly to obtain than harmonic frequencies for the same species.<sup>30</sup>

Anharmonic frequency calculations were performed on the lowest-energy isomer of the 5-FC–chloride cluster at the B3LYP/6-311+G(d,p) level of theory. Certain IR modes can be better approximated using an anharmonic oscillator approximation; however, for larger molecules or complexes, such calculations can be too costly.<sup>31–34</sup> Harmonic frequency values were used to obtain thermochemical values because of the tendency of anharmonic calculations to overestimate low-frequency quantities, leading to errors in calculated entropies and, consequently, Gibbs free energies.<sup>35</sup>

## RESULTS AND DISCUSSION

**Neutral and Protonated Isomers of 5-Fluorocytosine.** Four neutral isomers of 5-fluorocytosine were optimized at the B3LYP/6-311+G(d,p) level of theory and are shown in Figure 1.

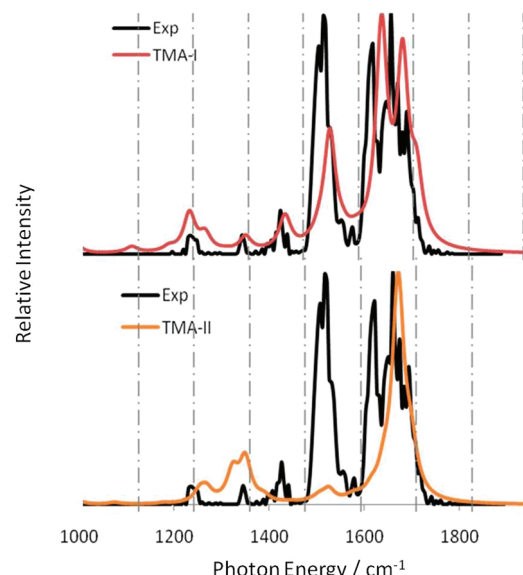


**Figure 5.** Comparison of the experimental spectrum with spectra (harmonic and scaled by 0.9679) calculated at the B3LYP/6-311+G(d,p) level of theory for several isomers of the trimethylammonium–5-fluorocytosine cluster. The experimental spectrum is represented in black, with the calculated spectra shown in color.

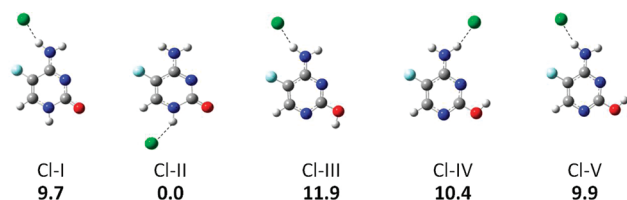


**Figure 6.** Structures and relative Gibbs free energies [ $\Delta G^\circ(298\text{ K})$ ] for several isomers of the chloride–5-fluorocytosine cluster. Structures were optimized at the B3LYP/6-311+G(d,p) level of theory, and relative Gibbs free energies (kJ/mol) were calculated at the B2PLYP/aug-cc-pVTZ//B3LYP/6-311+G(d,p) level of theory.

The lowest-energy isomer, Neutral-III, adopts a lactim-type structure that facilitates aromaticity in the ring system. The next two most favorable isomers, Neutral-I and -IV, lie close in Gibbs free energy (298 K) relative to Neutral-III at 6.2 and 4.2 kJ/mol, respectively. The significantly higher Gibbs free energy (298 K) of Neutral-II (40.3 kJ/mol) relative to those of Neutral-I, -III, and -IV suggests that its abundance should be negligible under the experimental conditions.

The formation of a cationic dimer can occur by the association of one neutral and one protonated 5-fluorocytosine molecule; therefore, protonated 5-fluorocytosine isomers were also considered and optimized at the B3LYP/6-311+G(d,p) level of theory. Each site of protonation on the neutral isomers of 5-FC shown in Figure 1 yielded two isomers that can be considered experimentally accessible. These two protonated isomers are shown in Figure 2. The lowest-energy isomer of protonated 5-FC, Protonated-II, adopts a lactam-type configuration. The only other low-energy isomer, Protonated-I, has a lactam-type structure and is 12.4 kJ/mol higher in Gibbs free energy (298 K) relative to Protonated-II. All other calculated isomers for protonated 5-FC were in excess of 30 kJ/mol higher in Gibbs free energy (298 K) relative to Protonated-I and were not considered for adduct formation.

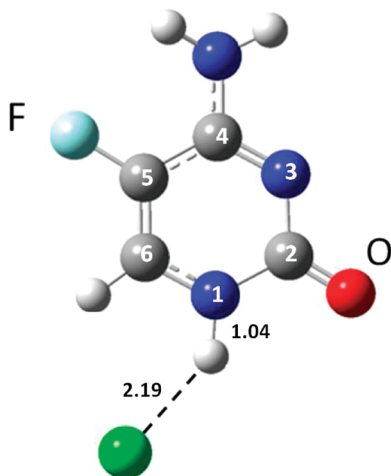
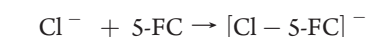


**Figure 7.** Structure of the lowest-energy chloride–5-fluorocytosine isomer, Cl-II, calculated at the B3LYP/6 + 311+G(d,p) level of theory. The ionic hydrogen bond is represented as a black dotted line. Bond lengths are in units of angstroms (Å).

**Table 2. Thermochemical Values (298 K) for the Formation of Several Chloride–5-FC Isomers Calculated at the B2PLYP/aug-cc-pVTZ//B3LYP/6-311+G(d,p) Level**



reaction scheme	$\Delta H^\circ$ (kJ/mol)	$\Delta S^\circ$ [J/(mol K)]	$\Delta G^\circ$ (kJ/mol)
$\text{Cl}^- + \text{Neutral-I} \rightarrow \text{Cl-I}$	-95.3	-93.3	-67.5
$\text{Cl}^- + \text{Neutral-I} \rightarrow \text{Cl-II}$	-107	-99.5	-77.1
$\text{Cl}^- + \text{Neutral-III} \rightarrow \text{Cl-III}$	-87.3	-94.9	-59.0
$\text{Cl}^- + \text{Neutral-IV} \rightarrow \text{Cl-IV}$	-91.4	-89.8	-64.7
$\text{Cl}^- + \text{Neutral-IV} \rightarrow \text{Cl-V}$	-92.1	-93.3	-65.2

**5-Fluorocytosine–Trimethylammonium Cluster.** Trimethylammonium (TMA) was chosen to cluster with 5-fluorocytosine because it can provide a model for cationic interactions with 5-FC that might be found biologically. A set of calculated lowest-energy isomers for the cluster formed by 5-FC and trimethylammonium is shown in Figure 3. Comparison of the relative Gibbs free energies (298 K) of these isomers suggests TMA-I (Figure 4) to be dominant in abundance during the experiments. TMA-I is bound by an ionic hydrogen bond formed between trimethylammonium and the carbonyl oxygen of 5-fluorocytosine. The proton affinity of 5-fluorocytosine was calculated to be 941 kJ/mol [B2PLYP/aug-cc-pVTZ//B3LYP/6-311+G(d,p)], and the established proton affinity for trimethylamine is 948.9 kJ/mol.<sup>36</sup> The calculated distances between the proton and the oxygen of 5-FC and between the proton and the nitrogen on trimethylammonium are 1.59 and 1.07 Å, respectively, suggesting that the proton lies closer to trimethylamine than to 5-fluorocytosine.

During many of the optimization procedures, starting structures of several additional isomers converged, through proton-transfer tautomerism, to structure TMA-I, the lowest-energy isomer. All other calculated species for the trimethylammonium–5-FC cluster were found to have relative Gibbs free energies (298 K) in excess of 27 kJ/mol compared to TMA-I and were therefore considered

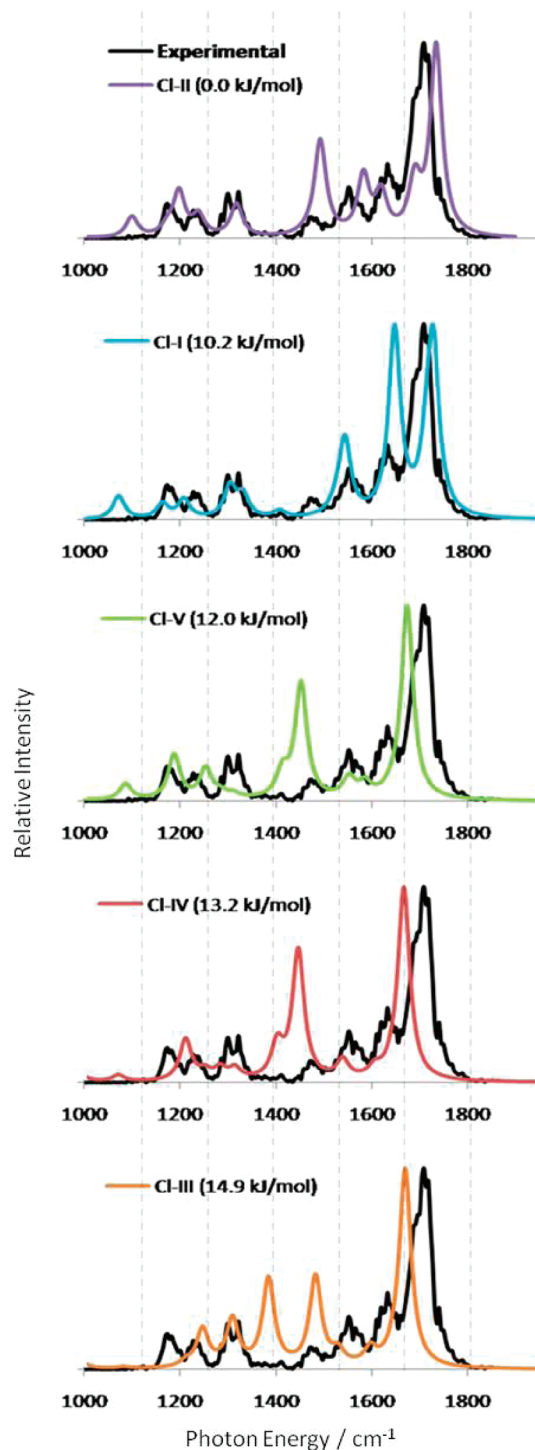


**Figure 8.** Comparison of the experimental spectrum with spectra (harmonic and scaled by 0.9679) calculated at the B3LYP/6-311+G(d,p) level of theory for several isomers of the chloride–5-fluorocytosine cluster. The experimental spectrum is represented in black, with the calculated spectra shown in color.

to exist at negligible concentrations under the experimental conditions. Indeed, assuming a Boltzmann distribution of internal energies, isomers with Gibbs free energy values in excess of 15 kJ/mol relative to the lowest-energy isomer might be considered to be statistically available in a ratio of 1:424, thus justifying this approach. The calculated values of Gibbs free energies of formation

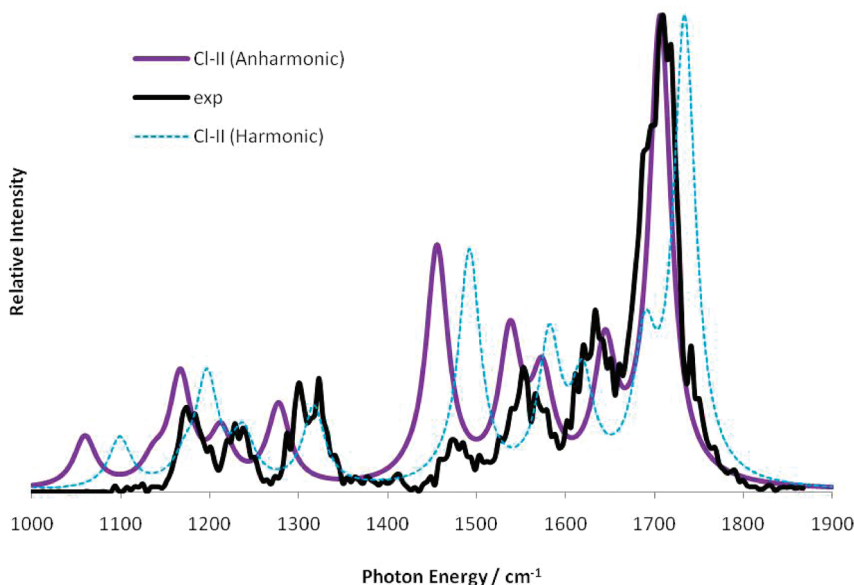


**Figure 9.** Harmonic and anharmonic calculated spectra in comparison with the experimental spectrum for the lowest-energy isomer of the chloride–5-fluorocytosine cluster, Cl-II. Harmonic (scaled by 0.9679) and anharmonic spectra were calculated using the B3LYP/6-311+G(d,p) level of theory.

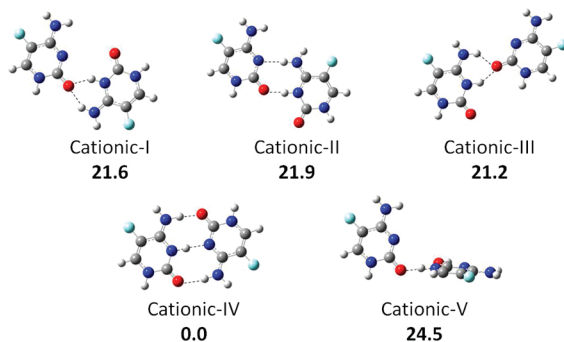


**Figure 10.** Structures and relative Gibbs free energies (298 K) for several isomers of the 5-fluorocytosine cationic dimer. Structures were optimized at the B3LYP/6-311+G(d,p) level of theory, and relative Gibbs free energies (kJ/mol) were calculated at the B2PLYP/aug-cc-pVTZ//B3LYP/6-311+G(d,p) level of theory.

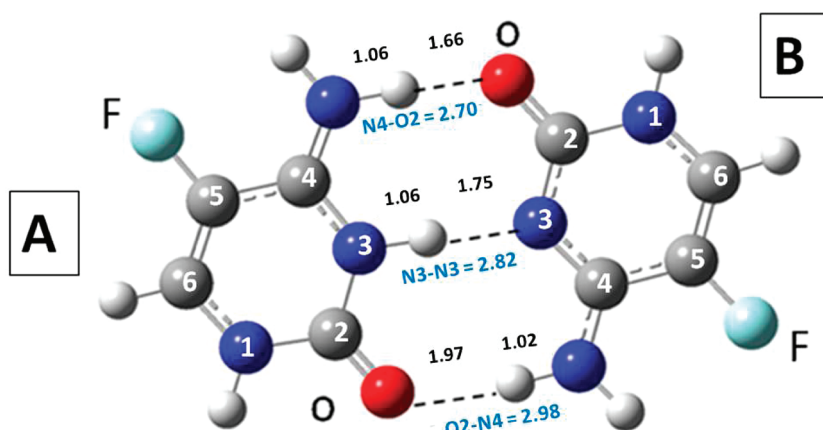
at 298 K [ $\Delta G^\circ(298\text{ K})$ ] for several trimethylammonium–5-FC clusters are listed in Table 1.

Figure 5 shows a comparison of experimental and calculated (TMA-I) spectra for the trimethylammonium–5-FC cluster. In the experimental spectrum, significant peaks arise at  $1621$  and  $1660\text{ cm}^{-1}$ , which are revealed by computational analysis to be due to the  $\text{R}'-\text{C}_2=\text{O}\cdots\text{H}-\text{N}^+\text{R}_3$  carbonyl stretch in asymmetric motion with the proton of trimethylammonium. These peaks were found to match well in the calculated (TMA-I) and experimental spectra and strongly suggest that TMA-I is the species being observed in experiments. In addition, vibrational spectra for higher-energy calculated species, such as TMA-II and TMA-III, have peaks indicating alternate interactions between 5-FC and trimethylammonium and do not approximate the experimental spectrum as closely. For example, the large peak at  $1478\text{ cm}^{-1}$  in the calculated TMA-II spectrum corresponds to the proton on trimethylammonium rocking between N1 of 5-FC and the nitrogen on trimethylammonium, and this peak is blue-shifted in comparison to peaks found in the experimental spectrum.

Overall, the calculated TMA-I spectrum matches the IRMPD spectrum rather well and shows that an ionic hydrogen-bonding interaction in the trimethylammonium–5-FC cluster occurs between the carbonyl oxygen of 5-fluorocytosine and the nitrogen of trimethylammonium.

**5-Fluorocytosine–Chloride Cluster.** Chloride was chosen to cluster with 5-fluorocytosine because it can provide a model for anionic interactions with 5-FC that might be found biologically. Optimized isomers of the chloride–5-FC cluster are shown in Figure 6. Comparison of the relative Gibbs free energies (298 K) of these species suggests that five isomers can be considered experimentally accessible: Cl-II, the lowest-energy isomer (Figure 7), along with Cl-I, -III, -VII, and -IV. Isomer Cl-II situates the chloride ion farthest from the electronegative heteroatoms in the molecule and contains an ionic hydrogen-bonding interaction between the chloride ion and  $\text{H}-\text{N}^-$  with a distance of  $2.19\text{ \AA}$ . In the other four relevant structures, chloride is in association with the amino group of 5-FC, and this difference consequently yields a unique vibrational spectrum for Cl-II. The calculated Gibbs free energies of formation at 298 K [ $\Delta G^\circ(298\text{ K})$ ] for several chloride–5-FC isomers are listed in Table 2.

Figure 8 presents the experimental and calculated spectra of the chloride–5-FC cluster. The calculated spectrum of the lowest-energy isomer, Cl-II, closely matches the experimental spectrum and indicates that Cl-II is likely the most prevalent isomer found in experiments. The calculated peaks at  $1197$  and  $1317\text{ cm}^{-1}$  arise from  $-\text{N}^-\text{H}$  and  $-\text{C}_6=\text{H}$  in-plane bending in the presence of the chloride ion. In addition, carbonyl stretching and  $\text{NH}_2$  scissoring modes are calculated at  $1734$  and  $1618\text{ cm}^{-1}$ , respectively. The calculated Cl-I spectrum is also a close match to the experimental spectrum. In this isomer, the carbonyl stretch is apparent at  $1728\text{ cm}^{-1}$ , along with the  $\text{Cl}\cdots\text{NH}_2$  scissoring at  $1647\text{ cm}^{-1}$ . The experimentally observed peak at approximately  $1450\text{ cm}^{-1}$ , however, does not appear in the Cl-I spectrum. This peak likely arises from the interaction between chloride and  $-\text{N}^-\text{H}$ , as observed in the Cl-II calculated spectrum. Nevertheless, based on the calculated energetics, it is probable that isomer Cl-I also exists to some extent under the experimental conditions.



**Figure 11.** Lowest-energy isomer for the 5-fluorocytosine cationic dimer, Cationic-IV, calculated at the B3LYP/6-311+G(d,p) level of theory. Hydrogen-bonding interactions are represented by black dotted lines. Bond lengths are reported in units of angstroms ( $\text{\AA}$ ).

**Table 3. Thermochemical Values (298 K) for Formation of Several Isomers of the 5-Fluorocytosine Cationic Dimer Calculated at the B2PLYP/aug-cc-pVTZ//B3LYP/6-311+G(d,p) Level**



reaction scheme	$\Delta H^\circ$ (kJ/mol)	$\Delta S^\circ$ [J/(mol K)]	$\Delta G^\circ$ (kJ/mol)
Neutral-I + Protonated-I	-154	-145	-78.1
→ Cationic-I			
Neutral-I + Protonated-I	-154	-148	-77.7
→ Cationic-II			
Neutral-I + Protonated-II	-141	-142	-66.0
→ Cationic-III			
Neutral-I + Protonated-I	-187	-184	-99.7
→ Cationic-IV			
Neutral-IV + Protonated-II	-130	-140	-60.7
→ Cationic-V			

For isomers Cl-V, -IV, and -III, the oxygen atom is not present in the carbonyl form and has chloride associating with the amino group of 5-FC. The spectra corresponding to these isomers contain no carbonyl peak; however, a comparatively shifted peak in the region of  $1700 \text{ cm}^{-1}$  is present from the  $\text{Cl}\cdots\text{NH}_2$  scissoring. Each of the spectra relating to Cl-V, -IV, and -III also contains a peak at approximately  $1500 \text{ cm}^{-1}$ , representing a bending motion within the enol functionality. In addition, Cl-V, specifically, does not account for a peak found experimentally at  $1316 \text{ cm}^{-1}$ , which likely corresponds to the in-plane rocking of  $-\text{C}_6\text{H}$  and the  $-\text{N}1\text{--H}$  interaction with the chloride ion.

Figure 9 shows the calculated harmonic and anharmonic spectra of Cl-II in comparison with the experimental spectrum. The vibrational modes at higher photon energies appear to be better approximated by the anharmonic calculation, whereas the vibrational modes at lower photon energy might be more harmonic in nature. Nevertheless, the calculated anharmonic spectrum is visibly red-shifted from the harmonic spectrum and, thus, for many vibrational modes, allows for a better approximation of the experimental spectrum.<sup>31–34</sup>

**5-Fluorocytosine Cationic Dimer.** The cationic dimer of 5-fluorocytosine is composed of one protonated species and

one neutral species interacting through ionic hydrogen-bonding interactions. In this work, monodentate, bidentate, and tridentate interactions were considered and optimized, in addition to both planar and nonplanar complexes. (Some relevant isomers are shown in Figure 10.) The calculated relative energetics of these optimized structures strongly indicate Cationic-IV (Figure 11), a planar complex containing a tridentate interaction, should predominate under the experimental conditions. The tridentate ionic hydrogen-bonding interaction found in this species is distinct because of the linear arrangement of the three ionic hydrogen bonds, leading to a very large calculated binding energy. Currently, the strongest known ionic hydrogen bond is found in the bisfluoride ion,  $\text{FHF}^-$ , with an experimentally determined binding energy of  $-192 (\pm 6.7) \text{ kJ/mol}$ .<sup>37</sup> We calculated the binding energy for Cationic-IV to be  $180 \text{ kJ/mol}$  [B2PLYP/aug-cc-pVTZ//B3LYP/6-311+G(d,p)], suggesting that Cationic-IV might be a contender among some of the strongest ionic hydrogen bonds known. The magnitude of the calculated binding energy associated with this unique tridentate interaction suggests that the ionic hydrogen bonds involved in the formation of Cationic-IV are very strong.

Calculated Gibbs free energies of formation at 298 K [ $\Delta G^\circ(298 \text{ K})$ ] for several cationic dimer isomers are included in Table 3. Calculated bond lengths, relating to the three ionic hydrogen bonds of Cationic-IV, are shown in Figure 11. The ionic hydrogen bond  $-\text{C}_{4A}\text{--NH--H}\cdots\text{O}=\text{C}_{2B}-$  has the shortest distance from heteroatom to heteroatom, suggesting that it is the strongest of the three ionic hydrogen bonds. In comparison, the  $-\text{N}_{3A}\text{--H}\cdots\text{N}_{2B}-$  and  $\text{C}_{2A}\text{=O}\cdots\text{H--HN--C}_{4B}-$  ionic hydrogen bonds grow subsequently longer by 0.12 and 0.28  $\text{\AA}$ , respectively.

Experimental and calculated vibrational spectra for several isomers of the 5-FC cationic dimer are shown in Figure 12. Several isomers of this species are very similar in structure and therefore have comparable calculated vibrational spectra; however, of the isomers considered, Cationic-IV was found to be the most energetically relevant. Cationic-III has a relative Gibbs free energy of  $21.2 \text{ kJ/mol}$  in comparison to Cationic-IV and is the next-lowest-energy isomer. Although several isomers might be present under the experimental conditions, Cationic-IV should be the most abundant. The peak assignments corresponding to the calculated Cationic-IV spectrum are shown in Table 4.

**Table 4.** 5-Fluorocytosine Cationic-IV Vibrational Spectrum Peak Assignments

peak(s) (cm <sup>-1</sup> )	atoms involved	assignment
1237	NH <sub>2</sub> —C4 <sub>B</sub> —	NH <sub>2</sub> in-plane rocking
1303	NH <sub>2</sub> —C4 <sub>A</sub> —	NH <sub>2</sub> in-plane rocking
1517, 1576, 1738	NH <sub>2</sub> —C4 <sub>A</sub> — —N3 <sub>A</sub> ···H···N3 <sub>B</sub> —	NH <sub>2</sub> in-plane rocking orthogonal proton motion
1540	NH <sub>2</sub> —C4 <sub>B</sub> —	NH <sub>2</sub> in-plane rocking
1558	—N3 <sub>A</sub> ···H···N3 <sub>B</sub> —	orthogonal proton motion
1647, 1716	NH <sub>2</sub> —C4 <sub>A</sub> —, NH <sub>2</sub> —C4 <sub>B</sub> — —N3 <sub>A</sub> ···H···N3 <sub>B</sub> —	NH <sub>2</sub> in-plane rocking orthogonal proton motion
1671	NH <sub>2</sub> —C4 <sub>B</sub> — N3 <sub>A</sub> ···H···N3 <sub>B</sub> —	NH <sub>2</sub> in-plane rocking orthogonal proton motion
1738	C2 <sub>B</sub> =O, C2 <sub>A</sub> =O	symmetric carbonyl stretch
1815	C2 <sub>A</sub> =O—	carbonyl stretch
	N3 <sub>A</sub> ···H···N3 <sub>B</sub> —	orthogonal proton motion

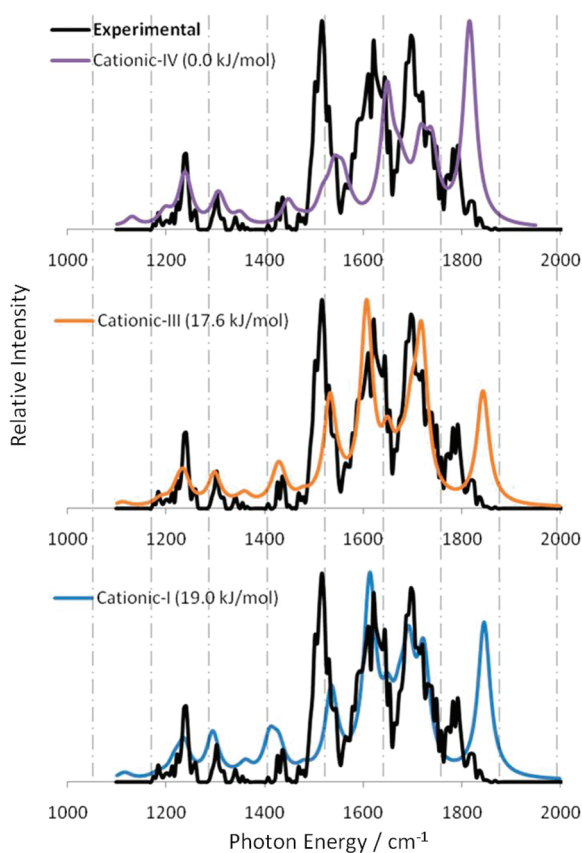


**Figure 12.** Comparison of the experimental spectrum with spectra (harmonic and scaled by 0.9679) calculated at the B3LYP/6-311+G(d,p) level of theory for several isomers of the cationic 5-FC dimer. The experimental spectrum is represented in black, with the calculated spectra shown in color.

## CONCLUSIONS

IRMPD spectroscopy in combination with electronic structure calculations has again been demonstrated here to be a valuable tool for structural elucidation. For each of the 5-fluorocytosine analogues considered, a single predominant species has been proposed. The B3LYP/6-311+G(d,p) level of theory

used for all geometry optimizations provided calculated spectra that approximate the experimental spectra well in most cases and, thus, also facilitated the characterization of each species of interest. Single-point calculations at the B2PLYP/aug-cc-pVTZ level of theory were used to more accurately approximate the electronic energies of each of the systems investigated and, thus, should provide more accurate thermochemical values.

Trimethylammonium was found to associate with 5-fluorocytosine at the carbonyl oxygen of 5-FC, as observed in isomer TMA-I (Figure 4). The proton involved in the ionic hydrogen-bonding interaction of this cluster was calculated to reside closer to the nitrogen of trimethylamine than the oxygen atom of 5-FC. The calculated spectrum for TMA-I has significant peaks at 1621 and 1660 cm<sup>-1</sup>, corresponding to the carbonyl stretch in asymmetric motion with the proton of trimethylammonium. Calculated spectra of the higher-energy isomers of the trimethylammonium–5-FC clusters yielded peaks that were shifted from the experimental spectrum, because of their ionic hydrogen-bonding interactions occurring at alternate sites. Overall, the calculated spectrum of TMA-I matches the experimental spectrum rather well.

For the cluster involving chloride in association with 5-fluorocytosine, a set of potentially relevant isomers was identified based on their relative energetics. The calculated spectrum for the lowest-energy isomer, Cl-II, qualitatively matches the experimental spectrum more so than the calculated spectra of the other isomers. The peak at around 1710 cm<sup>-1</sup> in the experimental spectrum appears to be from the carbonyl stretch and was found only in the calculated spectra of Cl-II and Cl-I, because, in the other isomers, the oxygen was not in carbonyl form. Because of their equally close match in calculated spectra, isomers Cl-II and Cl-I are likely to both be present in experiments; however, based on their relative energetics, Cl-II is likely to be most abundant.

The cationic dimer of 5-fluorocytosine was found to exist as a single dominant species with a very interesting tridentate ionic hydrogen-bonding interaction. The three ionic hydrogen bonds formed in this dimer were calculated to be very efficient and to result in an exceptionally large binding energy, with a value of 180 kJ/mol. Because of the similarity in structure of many of the lower-energy calculated isomers, the spectra for these species do not irrefutably identify the species being observed in experiments; however, the relative Gibbs free energies (298 K) of the 5-FC cationic dimers do indicate that Cationic-IV, which contains the tridentate ionic hydrogen-bonding interaction, should be the dominant isomer observed in experiments.

## ASSOCIATED CONTENT

**S Supporting Information.** Comprehensive lists of bond length, bond angle, and dihedral angle data for the lowest-energy isomer of each group of unique species described herein. All optimized parameters were calculated at the B3LYP/6-311+G(d,p) level of theory. This information is available free of charge via the Internet at <http://pubs.acs.org>

## AUTHOR INFORMATION

### Corresponding Author

\*Tel.: (519) 885-4567 ext. 36388 (S.M.M.), (519) 885-4567 ext. 84591 (T.B.M.). E-mail: s2marten@uwaterloo.ca (S.M.M.), mcmahon@uwaterloo.ca (T.B.M.).

## ■ ACKNOWLEDGMENT

The generous financial support of the Natural Sciences and Engineering Research Council of Canada (NSERC) is gratefully acknowledged, as is the financial support of the European Commission through the NEST/AVENTURE program (EPITO-PES, Project 15637). We are very grateful for the valuable assistance of the CLIO team, P. Maitre, J. Lemaire, J. M. Bakker, T. Besson, D. Scuderi, and J. M. Ortega, along with the CLIO technical support staff for their assistance during our stay in Orsay, France.

## ■ REFERENCES

- (1) Pai, M. P.; Bruce, H.; Felton, L. A. *Antimicrob. Agents Chemother.* **2010**, *54*, 1237.
- (2) Diasio, R. B.; Bennett, J. E.; Myers, C. E. *Biochem. Pharmacol.* **1978**, *27*, 703.
- (3) Ghannoum, M. A.; Rice, L. B. *Clin. Microbiol. Rev.* **1999**, *12*, 501.
- (4) Waldorf, A. R.; Polak, A. *Antimicrob. Agents Chemother.* **1983**, *23*, 79.
- (5) Murgich, J.; Franco, H. J.; San-Blas, G. *J. Phys. Chem. A* **2006**, *110*, 10106.
- (6) Desjardins, J.; Emerson, D. L.; Colagiovanni, D. B.; Abbott, E.; Brown, E. N.; Drolet, D. W. *J. Pharmacol. Exp. Ther.* **2004**, *309*, 894.
- (7) Boucher, P. D.; Im, N. M.; Freytag, S. O.; Shewach, D. S. *Cancer Res.* **2006**, *66*, 3230.
- (8) Lu, Y. C.; Luo, Y. P.; Wang, Y. W.; Tai, C. K. *Int. J. Mol. Med.* **2010**, *25*, 769.
- (9) Wu, R.; McMahon, T. B. *Mass Spectrom. Rev.* **2009**, *28*, 546.
- (10) Laskin, J.; Futrell, J. H. *Mass Spectrom. Rev.* **2005**, *24*, 135.
- (11) Wu, R. H.; McMahon, T. B. *J. Mass Spectrom.* **2008**, *43*, 1641.
- (12) Wu, R. H.; McMahon, T. B. *ChemPhysChem* **2008**, *9*, 2826.
- (13) Flora, J. W.; Muddiman, D. C. *J. Am. Chem. Soc.* **2002**, *124*, 6546.
- (14) Yoon, S. H.; Chamot-Rooke, J.; Perkins, B. R.; Hilderbrand, A. E.; Poutsma, J. C.; Wysocki, V. H. *J. Am. Chem. Soc.* **2008**, *130*, 17644.
- (15) Lemaire, J.; Boissel, P.; Heninger, M.; Mauclaire, G.; Bellec, G.; Mestdagh, H.; Simon, A.; Le Caer, S.; Ortega, J. M.; Glotin, F.; Maitre, P. *Phys. Rev. Lett.* **2002**, *89*, 273002.
- (16) Maitre, P.; Le Caer, S.; Simon, A.; Jones, W.; Lemaire, J.; Mestdagh, H.; Heninger, M.; Mauclaire, G.; Boissel, P.; Prazeres, R.; Glotin, F.; Ortega, J.-M. *Nucl. Instrum. Methods Phys. Res. A* **2003**, *507*, 541.
- (17) Marta, R. A.; Wu, R. H.; Eldridge, K. R.; Martens, J. K.; McMahon, T. B. *Phys. Chem. Chem. Phys.* **2010**, *12*, 3431.
- (18) Mac Aleese, L.; Simon, A.; McMahon, T. B.; Ortega, J. M.; Scuderi, D.; Lemaire, J.; Maitre, P. *Int. J. Mass Spectrom.* **2006**, *249*, 14.
- (19) Frisch, M. J.; Trucks, G. W.; Schlegel, H. B.; Scuseria, G. E.; Robb, M. A.; Cheeseman, J. R.; Montgomery, J. A., Jr.; Vreven, T.; Kudin, K. N.; Burant, J. C.; Millam, J. M.; Iyengar, S. S.; Tomasi, J.; Barone, V.; Mennucci, B.; Cossi, M.; Scalmani, G.; Rega, N.; Petersson, G. A.; Nakatsuji, H.; Hada, M.; Ehara, M.; Toyota, K.; Fukuda, R.; Hasegawa, J.; Ishida, M.; Nakajima, T.; Honda, Y.; Kitao, O.; Nakai, H.; Klene, M.; Li, X.; Knox, J. E.; Hratchian, H. P.; Cross, J. B.; Bakken, V.; Adamo, C.; Jaramillo, J.; Gomperts, R.; Stratmann, R. E.; Yazayev, O.; Austin, A. J.; Cammi, R.; Pomelli, C.; Ochterski, J. W.; Ayala, P. Y.; Morokuma, K.; Voth, G. A.; Salvador, P.; Dannenberg, J. J.; Zakrzewski, V. G.; Dapprich, S.; Daniels, A. D.; Strain, M. C.; Farkas, O.; Malick, D. K.; Rabuck, A. D.; Raghavachari, K.; Foresman, J. B.; Ortiz, J. V.; Cui, Q.; Baboul, A. G.; Clifford, S.; Cioslowski, J.; Stefanov, B. B.; Liu, G.; Liashenko, A.; Piskorz, P.; Komaromi, I.; Martin, R. L.; Fox, D. J.; Keith, T.; Al-Laham, M. A.; Peng, C. Y.; Nanayakkara, A.; Challacombe, M.; Gill, P. M. W.; Johnson, B.; Chen, W.; Wong, M. W.; Gonzalez, C.; Pople, J. A. *Gaussian 03*, revision C.02; Gaussian, Inc: Wallingford, CT, 2004.
- (20) Frisch, M. J.; Trucks, G. W.; Schlegel, H. B.; Scuseria, G. E.; Robb, M. A.; Cheeseman, J. R.; Scalmani, G.; Barone, V.; Mennucci, B.; Petersson, G. A.; Nakatsuji, H.; Caricato, M.; Li, X.; Hratchian, H. P.; Izmaylov, A. F.; Bloino, J.; Zheng, G.; Sonnenberg, J. L.; Hada, M.; Ehara, M.; Toyota, K.; Fukuda, R.; Hasegawa, J.; Ishida, M.; Nakajima, T.; Honda, Y.; Kitao, O.; Nakai, H.; Vreven, T.; Montgomery, J. A., Jr.; Peralta, J. E.; Ogliaro, F.; Bearpark, M.; Heyd, J. J.; Brothers, E.; Kudin, K. N.; Staroverov, V. N.; Kobayashi, R.; Normand, J.; Raghavachari, K.; Rendell, A.; Burant, J. C.; Iyengar, S. S.; Tomasi, J.; Cossi, M.; Rega, N.; Millam, J. M.; Klene, M.; Knox, J. E.; Cross, J. B.; Bakken, V.; Adamo, C.; Jaramillo, J.; Gomperts, R. E.; Stratmann, O.; Yazayev, A. J.; Austin, R.; Cammi, C.; Pomelli, J. W.; Ochterski, R.; Martin, R. L.; Morokuma, K.; Zakrzewski, V. G.; Voth, G. A.; Salvador, P.; Dannenberg, J. J.; Dapprich, S.; Daniels, A. D.; Farkas, O.; Foresman, J. B.; Ortiz, J. V.; Cioslowski, J.; Fox, D. J. *Gaussian 09*, revision A.1; Gaussian, Inc: Wallingford, CT, 2009.
- (21) Andersson, M. P.; Uvdal, P. *J. Phys. Chem. A* **2005**, *109*, 2937.
- (22) Bailey, C. L.; Mukhopadhyay, S.; Wander, A.; Harrison, N. M. *J. Phys. Conf. Ser.* **2009**, *100*, 1.
- (23) Szostak, E.; Druzbicki, K.; Mikuli, E. *J. Mol. Struct.* **2010**, *970*, 139.
- (24) Sierraalta, A.; Martorell, G.; Ehrmann, E.; Añez, R. *Int. J. Quantum Chem.* **2008**, *108*, 1036.
- (25) Arslan, H.; Algul, O. *Int. J. Mol. Sci.* **2007**, *8*, 760.
- (26) Zhao, D.; Langer, J.; Oomens, J.; Dopfer, O. *J. Chem. Phys.* **2009**, *131*, 184307.
- (27) Allen, R. N.; Lipkowski, P.; Shukla, M. K.; Leszczynski, J. *Spectrochim. Acta A* **2007**, *68*, 639.
- (28) Carl, D. R.; Cooper, T. E.; Oomens, J.; Steill, J. D.; Armentrout, P. B. *Phys. Chem. Chem. Phys.* **2010**, *12*, 3384.
- (29) Orio, M.; Pantazis, D. A.; Neese, F. *Photosynth. Res.* **2009**, *102*, 443.
- (30) Clabo, D. A.; Allen, W. D.; Remington, R. B.; Yamaguchi, Y.; Schaefer, H. F. *Chem. Phys.* **1988**, *123*, 187.
- (31) Chaban, G. M.; Jung, J. O.; Gerber, R. B. *J. Phys. Chem. A* **2000**, *104*, 10035.
- (32) Chaban, G. M.; Jung, J. O.; Gerber, R. B. *J. Phys. Chem. A* **2000**, *104*, 2772.
- (33) Buck, U.; Siebers, J.-G.; Wheatley, R. J. *J. Chem. Phys.* **1998**, *108*, 20.
- (34) Adesokan, A. A.; Gerber, R. B. *J. Phys. Chem. A* **2008**, *113*, 1905.
- (35) Njegic, B.; Gordon, M. S. *J. Chem. Phys.* **2006**, *125*, 224102.
- (36) Hunter, E. P. L.; Lias, S. G. *J. Phys. Chem. Ref. Data* **1998**, *27*, 413.
- (37) Wenthold, P. G.; Squires, R. R. *J. Phys. Chem.* **1995**, *99*, 2002.